Proceedings of the 1st Global Power and Propulsion Forum
GPPF 2017
Jan 16-18, 2017, Zurich, Switzerland
www.pps.global

GPPF-2017-186

ANALYTICAL STUDY OF COMBUSTION INSTABILITY IN SILO GAS TURBINE COMBUSTOR

S.Nosrati Shoar
MAPNA Turbine Engineering and Manufacturing Company (TUGA).
Nosrati.somayeh@mapnaturbine.com
Tehran, Iran

A.F. Tabatabaei
MAPNA Turbine Engineering and Manufacturing Company (TUGA).
Tabatabaei.abbas@mapnaturbine.com
Tehran, Iran

A.Ranjbaran
MAPNA Turbine Engineering and Manufacturing Company (TUGA).
Ranjbaran.Alireza@mapnaturbine.com
Tehran, Iran

ABSTRACT

Using the Low Nox systems in gas turbines in order to produce the minimum amount of Nox is done to reduce environmental pollution. Combustion instabilities are important problems occurring in industrial and aerial gas turbines with this system. If the heat release fluctuations and acoustic pressure are in the same phases, the amplitude of the fluctuations will increase. To study the dominant low frequency acoustic modes of an industrial silo gas turbine combustor, in a certain range of operating conditions, theoretical models are used in this study. This method leads to predictions for the frequencies of oscillations and the susceptibility to instabilities in which linear disturbances grow exponentially in time. The main components of the combustor model are assumed to be a plenum, burner, flame sheet, combustion chamber. This simplification is conceptually convenient since low frequency acoustic waves are not influenced by bends and some elements in the combustor are smaller than the wavelength of propagated acoustic perturbations. For the flame model the fuel is assumed to be injected in the burner at a steady rate. A convection time is assumed to characterize the required time for the acoustic velocity fluctuations to travel from the point of injection to the location of flame front in the combustion chamber. By applying proper boundary conditions between the components of combustor model, along with the combustor inlet and outlet boundary conditions, a system of equations can be obtained. This system of equations has a related eigenvalue equation which has complex roots. The sign of imaginary part of these roots determines whether disturbances grow or decay, and the real part of these roots gives the frequency of the modes. Acoustic mode shapes of the combustor are also studied by using COMSOL software and the other analytical method.

The results of calculated dominant acoustic frequencies which are obtained from theoretical models, simulated with COMSOL and measurements on operational gas turbines, show reasonable agreement

INTRODUCTION

Today's industrial gas turbines are designed to be more energy efficient and more reliable while they have to produce the minimum amount of NOx emission. For this purpose and to reduce the amount of NOx, low emission natural gas systems have been used. In order to decrease the amount of NOx emission a leaner fuel–air mixture should be used and this will lead to a lower flame temperature which consequently may result in heat release fluctuations. These heat release perturbations also may lead to combustion instability which is a major concern in the design process of industrial and aerial gas turbines.

In certain circumstances, the coupling between the generated heat release oscillations and acoustic pressure perturbations will result in specific low frequency instabilities, which is called humming. Humming emerges in high levels of dynamic pressure in the combustion chamber and it can prevent the system reaching its full load operating condition. Also it can result in dangerous damage to the internal components of combustion chamber. As a consequence, it can lead to decrease in the lifetime of the chamber or even failure of the whole structure. This phenomenon is a great barrier in development of gas turbines with premixed combustion capability using natural gas.

Hobson et al. [1], in a study conducted on a silo combustor, developed a theoretical model which has been used to derive some generic characteristics of combustion instability in terms of damping ratio.

Richards et al. [2-3] proposed a model for instability of a simple combustor based on the passive control method. In their study, the range of frequency of stability and the improvement in stability of combustor was investigated.

Schuermans et al. [4] studied a combustion system as a network of acoustic elements and based on their model the frequency of instability was obtained. They noted that it is necessary to include flame translation in the analytical model, of the flame response. Schuermans et al. [5] also investigated the limit cycle characteristics of combustion instabilities in annular combustion chambers.

Hubbard et al. [6] developed a low-order model to predict the frequency of oscillation and mode shape of gas turbine combustor.

Andreini et al. [7] developed a modular and mono-dimensional code (TA-1D), considering the linear acoustics analysis, to predict longitudinal resonance frequencies. They also performed a proper stability analysis for each obtained frequency and demonstrated the modal shapes of combustion chambers. Furthermore, several heat release models, such as a thin planar flame sheet or a conical flame shape, have been studied in their work. In their study [7], it has been reported that the capabilities of the code allow to extend the analysis to actual gas turbines.

Compa [8] also studied the thermoacoustic combustion instability, considering RANS simulations for modeling of the flame. His analysis was carried out by using commercial software, called COMSOL Multi-physics, based on the finite element methods. For the study of the nonlinear flame models, an acoustic network code (LOTAN) was also used. It has been reported [6] that the research was carried out through collaboration with Ansaldo Energia, which provided the geometry of the combustion chamber of the V94.3 machine.

According to the Rayleigh criterion [9], if the heat release and pressure fluctuations are in phase, this might boost the growth of oscillation's amplitude and could result in unpredicted behavior of the flame. Actually, the combustion instability are excited by feedback between the combustion process and acoustic oscillations that depends on system characteristics and operating conditions. It should be noted that the onset of instability is only a part of the problem of combustion instability. Accurate and complete understanding of the phenomenon requires the realization of mechanisms that are associated with the initiation and saturation of oscillations. Also according to studies of Lieuwen [10], some factors that might lead to occurrence of combustion instability are: (1) fuel feed line-acoustic coupling; (2) equivalence-ratio oscillation; (3) oscillatory atomization, vaporization and mixing. A significant amount of research in this area has been done. In spite of all these researches, yet little is known about the exact mechanisms and their sequences which may lead to occurrence of combustion instability. It has also been reported that equivalence ratio oscillation may result in perturbation of heat release through both direct and indirect mechanisms [11].

However, in this study we focus on prediction of unstable modes which could lead to the initiation of instabilities. The models that are used in this investigation could be applied to small linear oscillations. However, such linear models can provide useful information. This is because; if a mode is linearly stable it will not grow to form limit cycle. Furthermore, the frequency of linear modes usually provides a good approximation of the resulting limit cycle.

In this paper the thermoacoustic instability of a silo type combustor is investigated. For this purpose the main components of the combustor model are assumed to be a plenum, burner, flame sheet and combustion chamber. Acoustic matrices of all these subsystems are evaluated by means of thermodynamic conditions and flow speed. For instance, to model the acoustic behavior of the flame in terms of a transfer matrix, it is assumed that the acoustic and heat-release fluctuations at the flame front are coupled with fluctuations in the fuel–air mixture that are associated with acoustic disturbances at the fuel injectors. In other words, a convection time is considered to characterize the required time for the acoustic velocity fluctuations to travel from the point of injection to the location of flame front in the combustion chamber. By assembling the acoustic matrices of all subsystems, a model is generated which can predict the unstable frequency modes of the combustor. On the other hand, acoustic mode shapes of the combustor are also investigated by the COMSOL software.

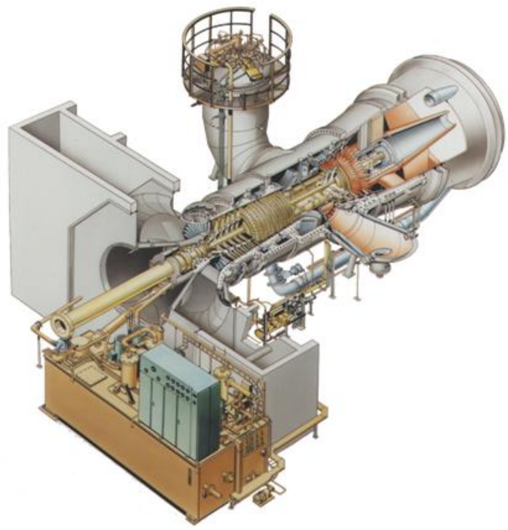

Figure 1: MGT-70 Gas Turbine

SILO COMBUSTOR MODELLING

Figure 2 shows a silo gas turbine combustor schematically. Plenum receives the combustion air which is conveyed from the compressor (not shown) and feeds it to a combustion chamber by passing the air through the outer surface of both the mixing chamber and flame tube. In some simplifications of the geometry, it has been assumed that there are two large chambers, representing the plenum and combustion chambers, which are connected by short premix ducts in which fuel is added to the air.

In this work the main subsystems of combustor are assumed to be: plenum, burner, flame sheet and combustion chamber. Combustion chamber is considered as well as a plenum. Using the upstream and downstream properties of mean flow, the transfer matrix of each subsystem can be determined. please add the transfer matrix of the combustion chamber

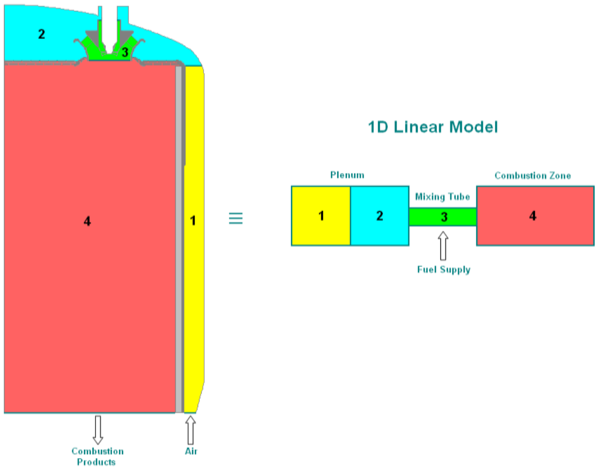

Figure 2: Schematic of flame tube in silo combustor and 1D Linear Model

PLENUM MODEL

We consider inviscid flow plenum transfer matrix between the mixing chamber and flame tube. The acoustic transfer matrices for various geometries are defined in[12]. For simple cylindrical elements:

$$R(s,L,\mu,f,c) = \begin{pmatrix} \cos(\frac{2\pi fL}{c}) & \frac{jc}{s}.\sin(\frac{2\pi fL}{c}) \\ \frac{js}{c}.\sin(\frac{2\pi fL}{c}) & \cos(\frac{2\pi fL}{c}) \end{pmatrix}.exp\left(-j\frac{\mu}{c}\frac{2\pi f}{c}L\right)$$

(1)

Transformation matrices for different geometries are defined in [12].

μ:bulk gas velocity m/s

c: sound velocity m/s

f: frequency

s: cross-sectional area

L: length

BURNER MODEL

The flow in the burner element is described by the unsteady, incompressible Bernoulli equation. In this model, the effect of unsteady fluctuations is associated with inertia work. Losses caused by the complex three-dimensional flow inside the burner are taken into account by using an integral loss coefficient and as a consequence the burner transfer matrix based on the [5] to be written.

$$\begin{pmatrix} p_2 \\ u_2 \end{pmatrix} = \begin{bmatrix} 1 & \rho_1 c_1 \left[M_1 (1-\varsigma-(\frac{A_1}{A_2})^2) - i\frac{\omega}{c_1} L_{red} \right] \\ 0 & \frac{A_1}{A_2} \end{bmatrix} \begin{pmatrix} p_1 \\ u_1 \end{pmatrix}, \quad (2)$$

where:

$$L_{red} = \int_0^1 \frac{A_0}{A(s)} ds = \int_0^1 \frac{u(s)}{u_0} ds, \quad (3)$$

ς = loss coeficient

The derivation of Eq.(2) is based on the assumption of compactness, that is, no physical length of the burner element would be considered in this study [5]. Actually for acoustic wavelengths that are much larger than burner dimensions the burner could be assumed as a compact element.

FLAME MODEL

In order to model the acoustic behavior of the flame, it is considered that the acoustic and heat-release fluctuations at the flame front are coupled with fluctuations in the fuel–air mixture that are attributable to acoustic disturbances at the fuel injectors. This implies the existence of a characteristic time lag τ after which the fuel particles reach the flame location on the other hand this model is based on a time delay. For fuel–air mixture φ and its fluctuation in time, the following relation can be written:

$$\frac{\varphi_1'(t)}{\varphi_1} = \frac{\varphi_i'(t-\tau)}{\varphi_i} \quad (4)$$

Whereas the heat release Q in the flame can be written as:

$$Q = \varphi_1 \rho_1 S_f h_{fuel} \quad (5)$$

In this work, the turbulent flame speed S_f is not assumed to be constant but is considered to be affected linearly by the fuel supply $S_f \sim \varphi$ which is reasonable for lean $\varphi < 1$ flames based on [5]. Consequently the fluctuations of heat release might be written as:

$$\frac{Q'}{Q} = 2\frac{\varphi_1'}{\varphi} + \frac{\rho_1'}{\rho_1} \quad (6)$$

By using the Rankine–Hugoniot jump conditions across the flame, the flame model can be formulated as:

$$\begin{bmatrix} 1 & \rho_1 c_1 (\frac{T_2}{T_1} - 1) M_1 (1 - e^{-i\omega\tau}) \\ 0 & (\frac{T_2}{T_1} - 1)(-e^{-i\omega\tau}) \end{bmatrix} \quad (7)$$

$$\begin{bmatrix} 1 & \rho_1 c_1 (\frac{T_2}{T_1} - 1) M_1 (1 - 2e^{-i\omega\tau}) \\ 0 & 1 - (\frac{T_2}{T_1} - 1)(2e^{-i\omega\tau}) \end{bmatrix} \quad (8)$$

With Two different flame models the same result was obtained in the predicted frequency of instability

ACOUSTIC TRANSFER MATRIX FOR A STEP EXPANSION

A step expansion (in the form of sudden area change) is placed at the interface between the burner exit and the combustor inlet. The heat release region is treated as a thin flame sheet located just downstream of this step expansion. The acoustic transfer matrix for step expansion is[12]:

$$\begin{bmatrix} 1 & M_2 Y_{02} \\ M_2/Y_{02} & 1 \end{bmatrix}\begin{bmatrix} P_2 \\ V_2 \end{bmatrix} =$$

$$\begin{bmatrix} 1-\frac{KM_1Y_1}{1-M_1^2} & \frac{KM_1Y_1}{1-M_1^2} \\ \frac{(\gamma-1)KM_1^3}{(1-M_1^2)Y_1} & 1-\frac{(\gamma-1)kM_1^2}{1-M_1^2} \end{bmatrix}\begin{bmatrix} 1 & M_1 Y_{01} \\ M_1/Y_{01} & 1 \end{bmatrix}\begin{bmatrix} P_1 \\ V_1 \end{bmatrix} \qquad (9)$$

BOUNDARY CONDITIONS

To study the effect of boundary conditions on thermoacoustic modes of combustor, various inlet and outlet boundary conditions, as shown in Table 1, were considered in this analysis. This code can be used in different boundary conditions. Depending on the type of combustion chamber the open boundary conditions to the inlet and outlet were considered.

Table 1 Combustion chamber boundary conditions[7].

Type	Boundary Condition	Acoustic Impedance
Open	$P^{/}=0$	$Z=0$
Closed	$u^{/}=0$	$Z=\infty$
Non-reflective		$Z=\pm1$
Choked outlet	$m^{/}$ = Constant	$2u^{/}/u + p^{/}/p - \rho^{/}/\rho = 0$
Choked Inlet	$m^{/}$ = Constant	$u^{/}/u + p^{/}/p = 0$

METHOD OF ANALYSIS

METHOD 1

All the transfer matrices can be combined into one system of equations, as shown in matrix.(10). The left-hand side of this equation consists of a large matrix that contains the transfer matrices of each subsystem and of a vector that contains the unknown pressures and velocities. The right-hand side of this equation contains the source terms.

```
M = [m_1_1,m_1_2,0,0,0,0,0,0,0,0,0,0,0,0,0,0,0,0,0,0,0,0,0,0,0,0,0,0;
    TM_TUBEA(1,1),TM_TUBEA(1,2),-1,0,0,0,0,0,0,0,0,0,0,0,0,0,0,0,0,0,0,0,0,
    TM_TUBEA(2,1),TM_TUBEA(2,2),0,-1,0,0,0,0,0,0,0,0,0,0,0,0,0,0,0,0,0,0,
    0,0,TM_STEP1(1,1),TM_STEP1(1,2),-1,0,0,0,0,0,0,0,0,0,0,0,0,0,0,0,0,
    0,0,TM_STEP1(2,1),TM_STEP1(2,2),0,-1,0,0,0,0,0,0,0,0,0,0,0,0,0,0,
    0,0,0,0,TM_ELBW1(1,1),TM_ELBW1(1,2),-1,0,0,0,0,0,0,0,0,0,0,0,0,0,0,0,0,
    0,0,0,0,TM_ELBW1(2,1),TM_ELBW1(2,2),0,-1,0,0,0,0,0,0,0,0,0,0,0,0,0,0,
    0,0,0,0,0,0,TM_TUBEB(1,1),TM_TUBEB(1,2),-1,0,0,0,0,0,0,0,0,0,0,0,0,0,0,
    0,0,0,0,0,0,TM_TUBEB(2,1),TM_TUBEB(2,2),0,-1,0,0,0,0,0,0,0,0,0,0,0,0,
    0,0,0,0,0,0,0,0,TM_Rvrs1(1,1),TM_Rvrs1(1,2),-1,0,0,0,0,0,0,0,0,0,0,0,0,
    0,0,0,0,0,0,0,0,TM_Rvrs1(2,1),TM_Rvrs1(2,2),0,-1,0,0,0,0,0,0,0,0,0,0,
    0,0,0,0,0,0,0,0,0,0,TM_STEP3(1,1),TM_STEP3(1,2),-1,0,0,0,0,0,0,0,0,0,0,
    0,0,0,0,0,0,0,0,0,0,TM_STEP3(2,1),TM_STEP3(2,2),0,-1,0,0,0,0,0,0,0,0,
    0,0,0,0,0,0,0,0,0,0,0,0,TM_TUBEC(1,1),TM_TUBEC(1,2),-1,0,0,0,0,0,0,0,0,
    0,0,0,0,0,0,0,0,0,0,0,0,TM_TUBEC(2,1),TM_TUBEC(2,2),0,-1,0,0,0,0,0,0,
    0,0,0,0,0,0,0,0,0,0,0,0,0,0,TM_STEP4(1,1),TM_STEP4(1,2),-1,0,0,0,0,0,0,
    0,0,0,0,0,0,0,0,0,0,0,0,0,0,TM_STEP4(2,1),TM_STEP4(2,2),0,-1,0,0,0,0,
    0,0,0,0,0,0,0,0,0,0,0,0,0,0,0,0,TM_FLAME(1,1),TM_FLAME(1,2),-1,0,0,0,0,
    0,0,0,0,0,0,0,0,0,0,0,0,0,0,0,0,TM_FLAME(2,1),TM_FLAME(2,2),0,-1,0,0,
    0,0,0,0,0,0,0,0,0,0,0,0,0,0,0,0,0,0,TM_TUBED(1,1),TM_TUBED(1,2),-1,0,0,0,
    0,0,0,0,0,0,0,0,0,0,0,0,0,0,0,0,0,0,TM_TUBED(2,1),TM_TUBED(2,2),0,-1,0,0,
    0,0,0,0,0,0,0,0,0,0,0,0,0,0,0,0,0,0,0,0,TM_STEP5(1,1),TM_STEP5(1,2),-1,0,
    0,0,0,0,0,0,0,0,0,0,0,0,0,0,0,0,0,0,0,0,TM_STEP5(2,1),TM_STEP5(2,2),0,-1,
    0,0,0,0,0,0,0,0,0,0,0,0,0,0,0,0,0,0,0,0,0,0,TM_ELBW2(1,1),TM_ELBW2(1,2),-
    0,0,0,0,0,0,0,0,0,0,0,0,0,0,0,0,0,0,0,0,0,0,TM_ELBW2(2,1),TM_ELBW2(2,2),0
    0,0,0,0,0,0,0,0,0,0,0,0,0,0,0,0,0,0,0,0,0,0,0,0,TM_TUBEE(1,1),TM_TUBEE(1,
    0,0,0,0,0,0,0,0,0,0,0,0,0,0,0,0,0,0,0,0,0,0,0,0,TM_TUBEE(2,1),TM_TUBEE(2,
    0,0,0,0,0,0,0,0,0,0,0,0,0,0,0,0,0,0,0,0,0,0,0,0,0,0,m_16_15,m_16_16];
```

(10)

The stability of the system can be assessed by analyzing the system's eigenvalues. The eigenvalues are frequencies for which the determinant of the large matrix (that contains the transfer matrices) vanishes. This determinant of large matrix can be solved by using a numerical root-finding procedure. If the imaginary parts of all roots are larger than zero, then the system is stable. If one or more roots have negative imaginary parts, then the system would be unstable. In addition, stability borders of the system as a function of the operation parameters, such as flame temperature, can also be determined.

A numerical-graphical method for solving the system of equations is used. The stability of the system can be assessed by analyzing the system's complex-valued eigenvalues. The eigenvalues are frequencies of instability for which the determinant of the matrix vanishes. Real and imaginary parts of determinant of matrix in the ranges of 0-100 Hz for frequency and 0-0.1 second for time lag are shown in Figures 3-6. The frequency of instability in this ranges is 80Hz. Figures 4 and 6 show a part of figures 3 and 5. This method is discussed in more detail in [13]

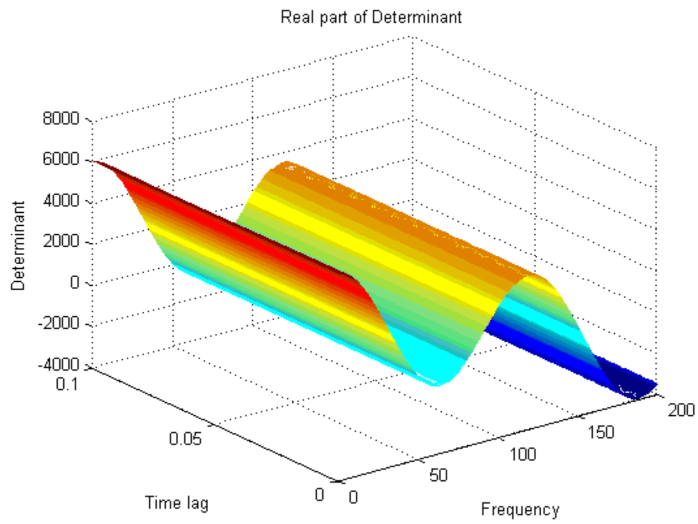

Figure 3: Real part of determinant of matrix vs frequency and time lag

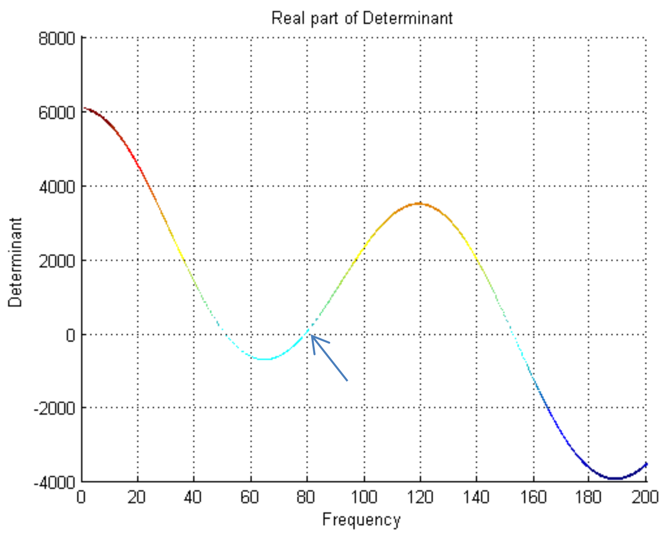

Figure 4: Real part of determinant vs frequency

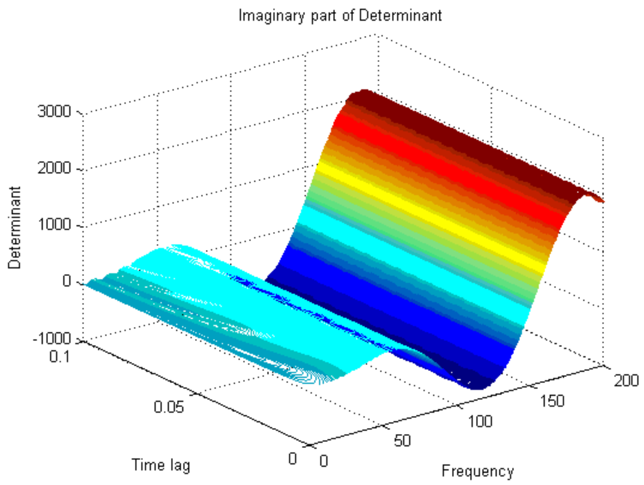

Figure 5: Imaginary part of determinant of matrix vs frequency and time lag

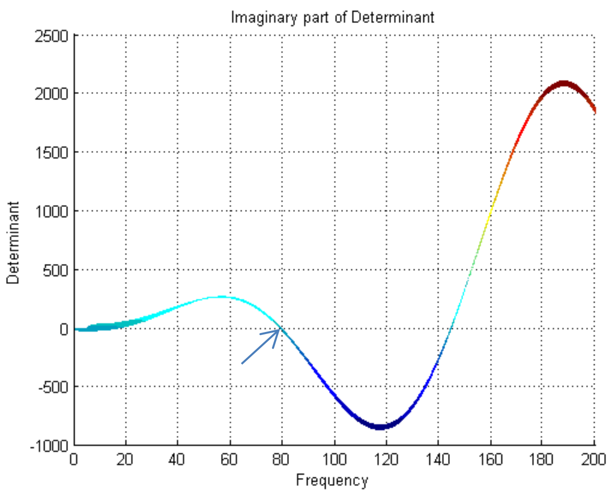

Figure 6: Imaginary part of determinant vs frequency

METHOD 2

Combustion instability is the result of an interaction between acoustic pressure fluctuation and heat-release perturbation. The feedback element (H) represent the conversion of heat-release variations into a pressure disturbance. The output signal from block H would represent the pressure produced in the flame region and in the references is shown how to calculate. [2] [14]

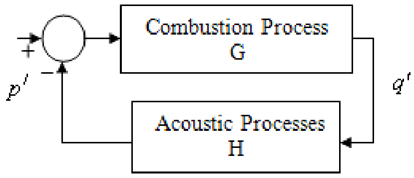

Figure 7: Block diagram of a dynamic thermoacoustic system

Fig.8 shows the variation of amplitude and phase of the system transfer function. Open loop response of the system is the product of G in H. Amplitude and phase of open loop responce is shown together in the above diagram in Figure 8. In the diagram below, just phase is shown. Where the amplitude of frequency is greater than one, and phase shift range is 90 to 180 degree there will be instability. This analysis indicates that the dominant modes of the system are around 80, 231 and 384 Hz.

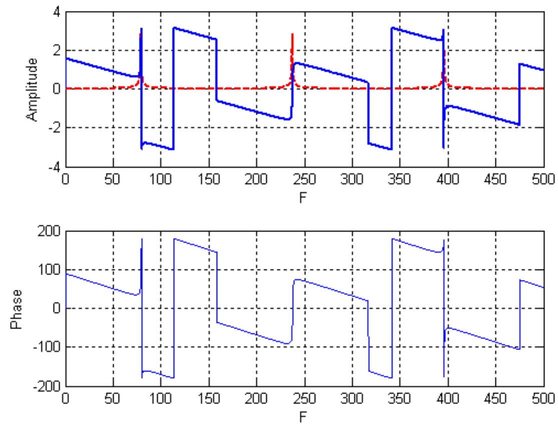

Figure 8: Amplitude and phase of the system transfer function versus frequency.

METHOD 3

This method is different to previous approaches. To start the calculations, average values of pressure, temperature and mass flow rate of flow at the inlet plenum chamber must be specified. Using these values, the mean flow parameters in parts of the first part and then the next, will be calculated. The calculations using the equations of conservation of mass and energy to various parts of the gas turbine can be done.[6]

$$\delta(S\overline{\rho u}) = 0 \tag{11}$$

$$\delta\left[(S\overline{\rho u})(c_p\overline{T} + \frac{1}{2}\overline{u}^2)\right] = \overline{Q} \tag{12}$$

When the average values were calculated in different parts of the gas turbine, the fluctuations of flow variables taken into consideration. The modeling of low-frequency fluctuations are concerned where only longitudinal waves are acoustic energy carrier. Equations in the variables respectively, pressure, velocity and density, in all regions 1 to 4 are written as follows.

$$p'(x,t) = e^{i\omega t}\left(Ae^{-i\omega x/c(1+M)} + Be^{i\omega x/c(1-M)}\right) \quad (13)$$

$$u'(x,t) = \frac{e^{i\omega t}}{\bar{\rho}c}\left(Ae^{-i\omega x/c(1+M)} - Be^{i\omega x/c(1-M)}\right) \quad (14)$$

$$\rho'(x,t) = \frac{p'(x,t)}{c^2} - \frac{S\bar{\rho}}{c_p}e^{i\omega(t-x/\bar{u})} \quad (15)$$

$$c_p T'(x,t) = \frac{p'(x,t)}{\bar{\rho}} + \frac{Sc^2}{(\gamma-1)c_p}e^{i\omega(t-x/\bar{u})} \quad (16)$$

$\omega = 2\pi f$

In order to calculate the flow parameters within the flame, average and fluctuation form of mass conservation equation, momentum and energy are written as follows:

$$\bar{\rho}_1 u_1' + \bar{u}_1\rho_1' = \bar{\rho}_2 u_2' + \bar{u}_2\rho_2' \quad (17)$$

$$p_1' + 2\bar{u}_1\bar{\rho}_1 u_1' + \rho_1'\bar{u}_1^2 = p_2' + 2\bar{u}_2\bar{\rho}_2 u_2' + \rho_2'\bar{u}_2^2 \quad (18)$$

$$\bar{\rho}_2\bar{u}_2\bar{H}_2 = \bar{\rho}_1\bar{u}_1\bar{H}_1 + \bar{Q} \quad (19)$$

$$\bar{\rho}_2\bar{u}_2\left[h_2' + \bar{u}_2 u_2'\right] = \bar{\rho}_1\bar{u}_1\left[h_1' + \bar{u}_1 u_1'\right] + Q' - \left(\bar{H}_2 - \bar{H}_1\right)\left(\bar{\rho}_1 u_1' + \bar{u}_1\rho_1'\right) \quad (20)$$

$$Where: \quad \bar{H} = \bar{h} + \frac{\bar{u}^2}{2} \;;\; h' = c_p T'; \quad (21)$$

$$\frac{\acute{Q}}{\bar{Q}} = -\frac{\acute{u}}{\bar{u}}e^{-i\omega(l+x)/\bar{u}} \quad (22)$$

In order to solve the matrix and get zeros, the Optimization Toolbox in MATLAB software is used. In this way, by putting the initial value corresponding to the desired range, may be the closest frequency to zero the determinant of the matrix obtained.

By applying assumptions in one-dimensional code execution, unstable and stable frequencies (due to sign of the imaginary part of the frequency stability is determined) obtained and mode shapes are plotted. The matrix is shown in appendix. In Figure 9, the amplitude of pressure fluctuations from the beginning of plenum to the end of the combustion chamber shown. A jump can be seen at the burner

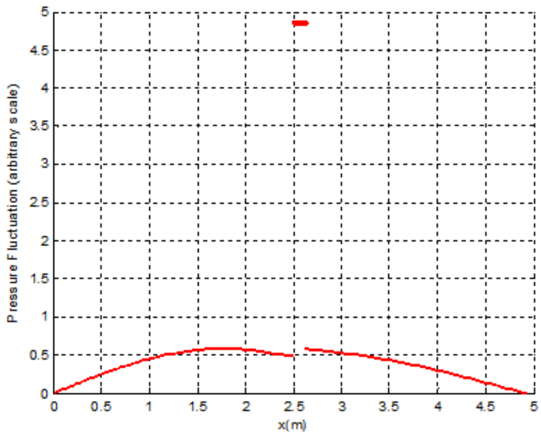

Figure 9: Mode shape for f=69.905-8.12i with open boundary condition at inlet and outlet

RESULTS

The geometry of the silo combustion chamber is created from real data. The geometry created at this stage is simplified compared to the main drawing. Some detailed parts are cut off, since their influence to the acoustical analysis is negligible. These simplifications are allowable because the dimensions of these elements are smaller than the dominant acoustic wavelength. Using COMSOL software the modeshapes of silo combustor were obtained and based on these results the dominant frequencies of system is studied. In this consideration entry boundary conditions due to hot combustion chamber are placed. Results show that the dominant longitudinal mode are 80 Hz. The first longitudinal acoustic mode of 80 Hz is shown in Figure 10. In Figure 11, the results of the frequency during the occurance of humming are shown. The results of the study, analytical methods, numerical methods and measurements are shown in Table 2. As can be seen, the third method has the least error.

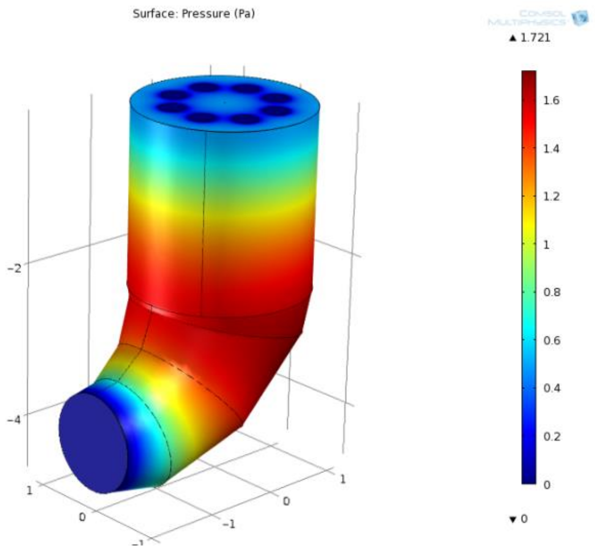

Figure 10. Acoustic modeshape of the combustor for frequency of 80 Hz

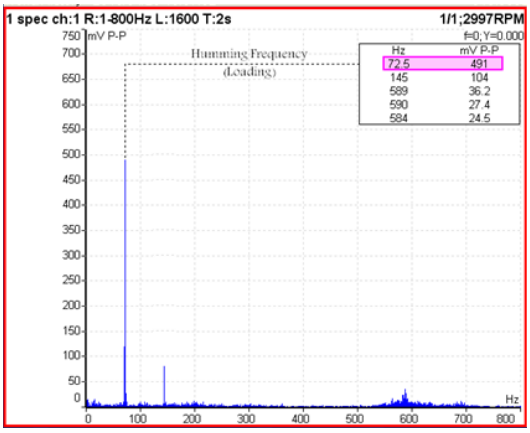

Figure 11: Frequency of humming by measurements

Table 2: Results of predicted frequency

Method	Frequency(Hz)
Hobson et al. [1]	78
Method 1 [4-5]	80
Method 2 [2-3]	79
Method 3 [6]	69.9
COMSOL	80
Measurements	72.5

CONCLUSIONS

This study, thermoacoustic modes of a silo combustor (MGT-70 heavy-duty gas turbine) were investigated using theoretical models together with COMSOL software. The frequencies associated with dominant acoustic modes of this combustor which are obtained from analytical models, measurment and simulation show a reasonable agreement. These frequencies are in the range of results which has been reported in previous studies [1] and is shown in table 2. The results of the analysis can be applied in the implementation of tuning to eliminate instability. In addition, the developed codes, in the early stages of the design and optimization of the combustion chamber of gas turbines will be used.

ACKNOWLEDGMENTS

The authors would like to show appreciation for Mapna Group's support of this study.

APPENDIX

```
e11 = exp((-2*1i*pi*l1*f(kk,jj))/(c1*(1+M1)));
e12 = exp((1i*2*pi*l1*f(kk,jj))/(c1*(1-M1)));
e21 = exp((-1i*2*pi*l1*f(kk,jj))/(c2*(1+M2)));
e22 = exp((1i*2*pi*l1*f(kk,jj))/(c2*(1-M2)));
e31 = exp((-1i*2*pi*(l1+l2)*f(kk,jj))/(c2*(1+M2)));
e32 = exp((1i*2*pi*(l1+l2)*f(kk,jj))/(c2*(1-M2)));
e41 = exp((-1i*2*pi*(l1+l2+l3)*f(kk,jj))/(c4*(1+M4)));
e42 = exp((1i*2*pi*(l1+l2+l3)*f(kk,jj))/(c4*(1-M4)));
e51 = exp((-1i*2*pi*(l1+l2+l3+l4)*f(kk,jj))/(c4*(1+M4)));
e52 = exp((1i*2*pi*(l1+l2+l3+l4)*f(kk,jj))/(c4*(1-M4)));


 M=[1,1,0,0,0,0,0,0,0,0;
   c2*s1*(1+M1)*e11, c2*s1*(M1-1)*e12, -c1*s2*(1+M2)*e21 ,
c1*s2*(1-M2)*e22,0,0,0,0,0,0;
   ((1+M1)^2)*e11,((1-M1)^2)*e12,-((1+M2)^2)*e21, -((1-
M2)^2)*e22,0,0,0,0,0,0;
  0,0,c3*s2*(1+M2)*e31, c3*s2*(M2-1)*e32,0,0,-c2*s3*M3, -
c2*c3*s3*ro3,0,0;
  0,0,0,0,c3*s4*(1+M4)*e41, c3*s4*(M4-1)*e42, -c4*s3*M3,-
c3*c4*s3*ro3,-c3*s4*M4,0;
  0,0,(s2*(1+M2)^2)*e31,(s2*(1-M2)^2)*e32, 0,0,-
s3*(1+M3^2),-2*ro3*s3*u3,0,0;
  0,0,0,0,s4*(1+M4)^2*e41,s4*(1-M4)^2*e42,-s3*(1+M3^2),-
2*ro3*s3*u3,-s4*M4^2,0;
  0,0,0,0,s4*(1+M4)*(u4+(cp*T04/c4))*e41,s4*(1-M4)*(u4-
(cp*T04/c4))*e42, -s3*M3*((c3+(cp*T03/c3))),-
s3*ro3*(u3^2+cp*T03),-s4*M4*((cp*T04/c4)-(c4/(gama2-1))),-
1;
  0,0,0,0,(2-M4*(gama2-1))*e51,-(2+M4*(gama2-1))*e52,0,0,-
M4,0;
  0,0,0,0,0,0,0,0,(q/u3)*exp(1i*2*pi*f(kk,jj)*t),0,1];
```

REFERENCES

[1] Hobson, D. E., Fackrell, J. E., Hewitt, G. “Combustion Instabilities in Industrial Gas Turbines- Measurments on Operating Plant and Thermoacoustic Modeling. Journal of Engineering for Gas Turbines and Power”, Vol. 122, No. 3, 2000, pp.420-428

[2] Richards, G. A., Straub, D. L., Robey, E. H., “Passive Control of Combustion Dynamics in Stationary Gas Turbine”, Journal of Propulsion and Power”, Vol 19, NO .5, 2003, pp795-810

[3] Richards, G. A., Straub, D. L., Robey, E. H., “Control of Combustion Dynamic Using Fuel System Impedance”, ASME GT2003-38521

[4] Schuermans, B. H., and Polifke. W., “Modeling Transfer Matrices of Premixed Flames and Comparison with Experimental Results”, American Society of Mechanical Engineers, Paper 99-GT-132.

[5] Schuermans, B. H., Paschereit, C. O., Monkewitz, P. “Non-linear Combustion Instabilities in Annular Gas-Turbine Combustors”, AIAA 2006-0549

[6] Hubbard, S., and Dowling, A.P., “Acoustic Resonances of an Industrial Gas Turbine Combustion System”, ASME Paper No. 2000-GT-94,

[7] Andreini, A. Facchini, B. Mangani, L. Simonetti, F. “Development And Validation of Tool For Thermoacoustic Instabilities Analysis In gas Turbine Combustors”. ASME GT2008-51248

[8] Compa, G., “Prediction of the Thermoacoustic Combustion Instability in Gas Turbine”, 2011,PHD Thesis, Politcnico di bari.

[9] Rayleigh.J. S. W., “The Theory of Sound”, Vol. 2, Dover, New York, 1945.

[10] Lieuwen, T. C., “Investigation Of Combustion Instability Mechanisms In Premixed Gas Turbines”, 1999,PHD. Thesis, Aersopace Engineering Department. Georgia Institute Technology.

[11] Cho, J. H. and Lieuwen, T. C., “Laminar Premixed Flame Response to Equivalence Ratio Oscillations”, Combustion and Flame, Vol. 140, 2005, pp. 116-129.

[12] Munjal, M. L., “Acoustics of Ducts and Mufflers”, John Wiley & Sons, 1986.

[13] Shuermans, B., and Paschereit, C.O., “ Investigation of Thermoacoustic Oscillations in combustion Systems using an Acoustic Network Model,” Acoustics of Combustion; EU-ROTHERM Seminar No. 67, Univ of Twente, Enschede, The Netherlands, July 2000.

[14] Lieuwen, T. C., Yang, V. “ Combustion Instabilities in Gas Turbine Engines: Operational Experience, Fundamental Mechanisms, and Modeling” University of Texas at Arlington, 2005